Geochemical Perspectives Letters

Loss of immiscible nitrogen from metallic melt explains Earth's missing nitrogen

J. Liu[1*], S.M. Dorfman[1*], M. Lv[1], J. Li[2], F. Zhu[2], Y. Kono[3,4]

OPEN ACCESS
doi: 10.7185/geochemlet.1919

Abstract

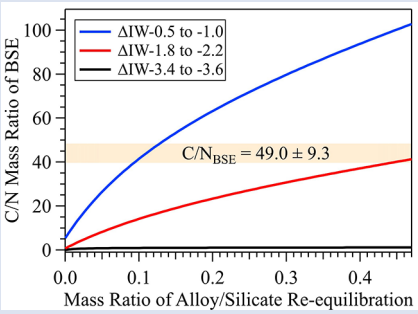

Nitrogen and carbon are essential elements for life, and their relative abundances in planetary bodies are important for understanding planetary evolution and habitability. The high C/N ratio in the bulk silicate Earth (BSE) relative to chondrites has been difficult to explain through partitioning during core formation and outgassing from molten silicate. Here we propose a new model that may have released nitrogen from the metallic cores of accreting bodies during impacts with the early Earth. Experimental observations of melting in the Fe-N-C system *via* synchrotron X-ray radiography of samples in a Paris-Edinburgh press reveal that above the liquidus, iron-rich melt and nitrogen-rich liquid coexist at pressures up to at least 6 GPa. The combined effects of N-rich supercritical fluid lost to Earth's atmosphere and/or space as well as N-depleted alloy equilibrating with the magma ocean on its way to the core would increase the BSE C/N ratio to match current estimates.

Received 2 January 2019 | Accepted 8 June 2019 | Published 30 July 2019

Introduction

The habitability of Earth and other planetary bodies depends on the incorporation, distribution, and speciation of volatile elements including carbon and nitrogen. In Earth, the BSE C/N ratio is estimated to be higher than that of planetary building blocks including enstatite, carbonaceous chondrites, interstellar dust and gas (*e.g.*, Marty, 2012; Bergin *et al.*, 2015). Recent studies estimate the BSE C/N ratio to be superchondritic based on measurements of gas bubbles trapped in mid-ocean ridge and ocean island basalts (Marty, 2012; Halliday, 2013; Bergin *et al.*, 2015), and recent estimates of the BSE C/N ratio converge to 49 ± 9 (Bergin *et al.*, 2015). In contrast, C/N ratios measured in primitive CI chondrites (17 ± 3; Alexander *et al.*, 2013) and enstatite chondrites (14 ± 12; Grady and Wright, 2003) are significantly lower. Explaining these observations thus requires one or more mechanisms that preferentially deplete N relative to C from the mantle source of basalt magmas.

The key processes responsible for C and N redistribution among Earth reservoirs were equilibrium partitioning between the magma ocean and the growing metallic core and degassing of the magma ocean to the early atmosphere, but these processes have been insufficient to explain the estimated high BSE C/N ratio (Bergin *et al.*, 2015; Hirschmann, 2016; Dalou *et al.*, 2017). Core formation is expected to decrease the BSE C/N ratio because at relevant conditions C is a much stronger siderophile element than N (*e.g.*, Dalou *et al.*, 2017). Degassing has not been thought to significantly affect the C/N ratio, as chemical analysis of volatiles in silicate glasses quenched from high pressure-temperature (*P-T*) experiments indicates that the solubilities of C and N in the magma ocean are comparable (Hirschmann, 2016).

The major host phase for both C and N in the solidifying planet is likely to be core-forming alloy, therefore understanding the Fe-N-C system under relevant conditions may hold the key to the paradox of the high BSE C/N ratio. While the Fe-C phase diagram has been well studied over a wide range of pressures (*e.g.*, Fei and Brosh, 2014; Liu *et al.*, 2016), very limited data are available on the phase relations of the Fe-N system (*e.g.*, Guillermet and Du, 1994). In particular, melting behaviours are expected to be different in these two systems, as the C-rich end member, graphite/diamond, has a melting point of 4000-5000 K at relevant pressures (Grumbach and Martin, 1996), while the N-rich end member would be gas/supercritical fluid in the BSE.

Immiscible N-rich Fluid

In order to test whether the mobility of N-rich gas/fluid could provide a possible mechanism to leak N during accretion and core formation, we investigated melting relations in the Fe-N-C system under high pressures by *in situ* X-ray radiography and

1. Department of Earth and Environmental Sciences, Michigan State University, MI 48824, USA
2. Department of Earth and Environmental Sciences, University of Michigan, MI 48109, USA
3. HPCAT, Geophysical Laboratory, Carnegie Institution of Washington, IL 60439, USA
4. Geodynamics Research Center, Ehime University, Ehime 790-8577, Japan
* Corresponding author (email: jiacliu09@gmail.com, dorfman3@msu.edu)

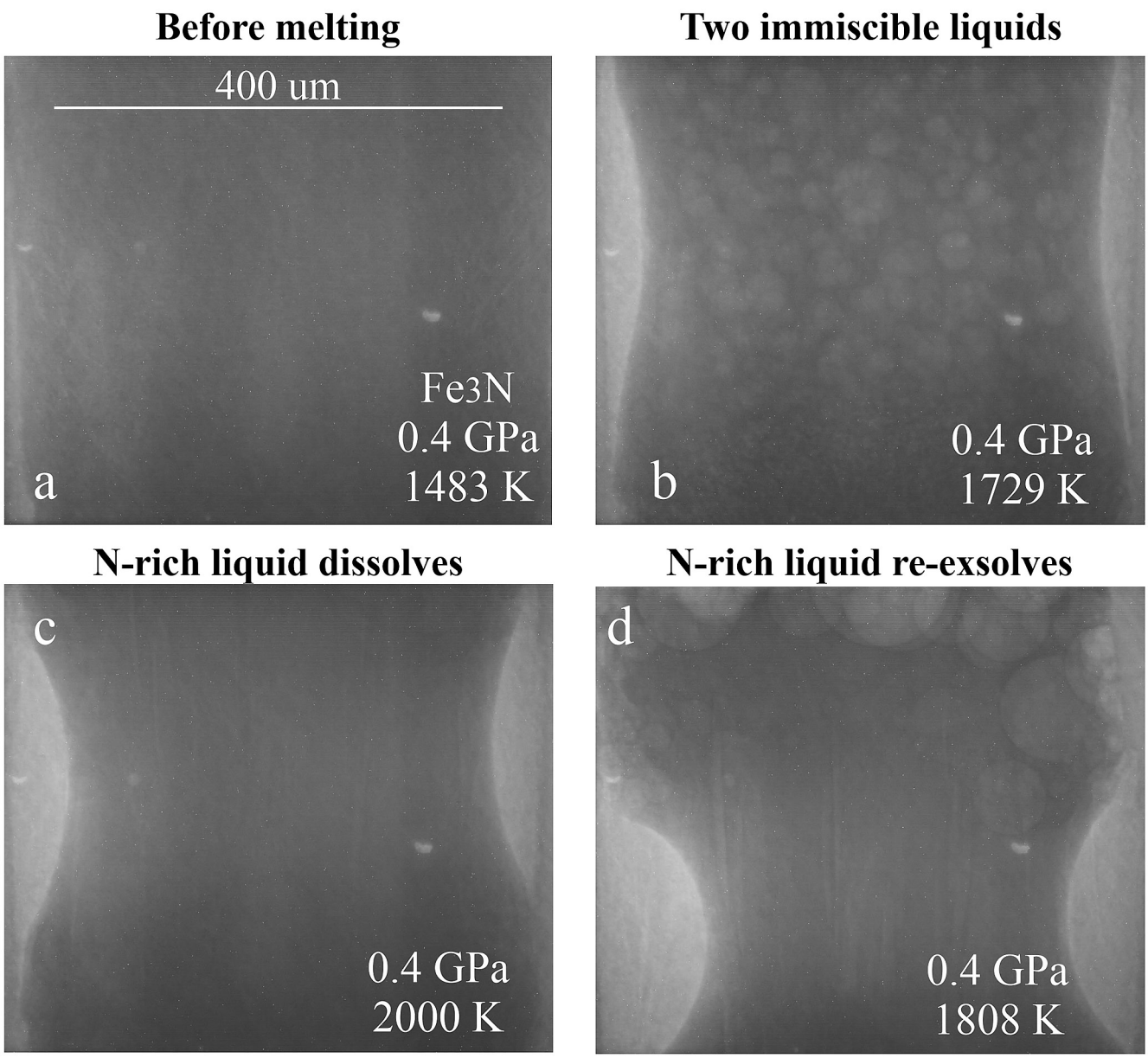

Figure 1 Representative X-ray radiographic images showing the evolution of the miscibility gap in Fe-N-C system under high pressure and high temperature conditions (run 4-17). This *in situ* X-ray radiography experiment starts at 0.4 GPa with Fe_3N as the starting material. **(a)** The sample is below solidus at 0.4 GPa and 1483 K. **(b)** Around 1729 K, immiscible N-rich supercritical fluid coexists with metallic liquid. **(c)** At higher temperatures, N-rich supercritical fluid partially dissolves into metallic liquid. **(d)** Lowering temperature re-exsolves N-rich supercritical fluid from metallic liquid. The corresponding movie is shown in Video S-1.

X-ray diffraction (XRD) coupled with Paris-Edinburgh (PE) cells and *ex situ* chemical analysis. The starting materials are either iron nitrides (Fe_3N and Fe_4N) or a mixture of iron and iron nitride powders with or without graphite powders. The starting N and C contents range from 0-7.7 wt. % and 0-10.0 wt. %, respectively (Table S-1). A standard PE sample assembly configuration was employed (Kono *et al.*, 2014), which used X-ray transparent MgO as the sample capsule and a cylindrical graphite tube outside sample capsule as the heater. Assemblages were first compressed to target pressures and gradually heated to be fully molten. Then the molten samples were quenched below 500 K within 5 seconds to preserve compositions for *ex situ* chemical analysis (Table S-1).

Below the solidus, starting materials for all runs were homogenous at ~3 mm spatial resolution of X-ray radiographic images (*e.g.*, Fig. 1a). An upper bound for the onset of partial melting at higher temperature was indicated by the appearance of 10s-micron regions of low X-ray absorption (*e.g.*, Fig. S-1b). At higher temperatures, these lighter regions merged to form 10s to 100s-micron droplets which moved vigorously (Fig. 1b). XRD patterns during heating also recorded the melting process (Fig. S-1d): at 0.4 GPa and 300 K, the XRD pattern confirmed Fe_3N as the starting material; at ~1690 K, most crystalline peaks disappeared an obvious increase in background at ~34-80 keV (Fig. S-1d), which originated from diffuse scattering signal. The corresponding X-ray radiographic image (Fig. S1-b) showed the ubiquitous occurrence of the low X-ray absorption regions. Therefore, both the XRD pattern and X-ray radiographic image indicated a partially molten state of the Fe-N sample. Turbulent flow of two phases occurred above ~1725 K (Video S-1), and the corresponding XRD pattern exhibited diffuse scattering with no XRD peaks (Fig. S-1d) and thus indicated conditions above the liquidus but below the solvus. At higher temperatures, the immiscible droplets partially dissolved into the metallic liquid but persisted to the highest temperature investigated in run 4-17 (~2000 K, Fig. 1c). Lowering temperature made more immiscible droplets

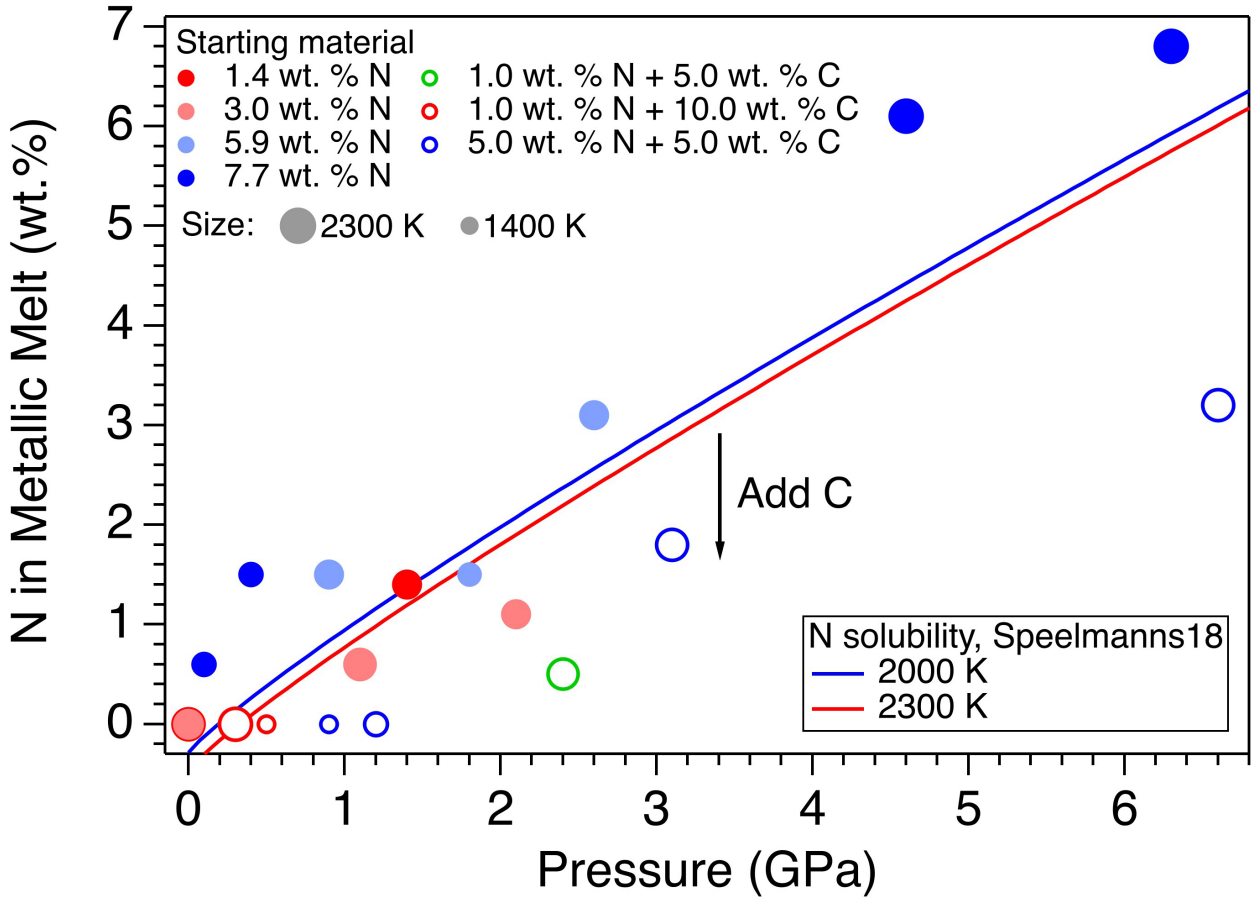

Figure 2 The pressure dependence of N solubility in Fe-N-C melt. The solid circles are for Fe-N starting materials; the open circles are for Fe-N-C starting materials. Symbol sizes are proportional to the temperatures (1400-2300 K) at which the experiments are quenched and colours indicate initial compositions (see legend). The blue and red curves are modelled N solubilities in Fe-N-C melt at 2000 K and 2300 K, respectively, from Speelmanns *et al.* (2018).

re-exsolve (Fig. 1d), confirming that the disappearance of the immiscible droplets from Figures 1b to 1c cannot be explained by loss of N-rich fluid through the MgO capsule. In comparison, no inhomogeneity appeared at all in Fe melting experiments at 0.8 GPa up to 2103 K (Fig. S-2).

The immiscible droplets with lighter colours in X-ray radiographic images are enriched in N because the contrast in X-ray radiographic images reflects density differences (Kono *et al.*, 2015). The N-rich nature of the immiscible fluid is confirmed by *ex situ* chemical analysis of the quenched samples: for experiments quenched with the presence of immiscible liquids, the regions which are lighter in X-ray radiographic images correspond to voids in recovered samples (*e.g.*, Figs. S-3 to S-6); N contents in the recovered samples are lower than the starting values when immiscible melting occurs (Table S-1). For example, N content in run 4-16 decreases from 5.9 % in the starting materials to 1.5 % in the recovered sample (Fig. S-3). With increasing temperature, the increase of N solubility in metallic melt (*e.g.*, Fig. 1 and Video S-1) can be explained by the concave-down shape of the solvus, which marks the phase boundary between one liquid and two immiscible liquids (Fig. S-7). A similar phenomenon has been observed in the Fe-O system (Kowalski and Spencer, 1995; Tsuno *et al.*, 2007): at 1 bar, O solubility increases from ~0 to ~5 mol. % when temperature increases from ~1811 K to ~2340 K (Kowalski and Spencer, 1995). Such a miscibility gap persists to at least 21 GPa in the Fe-O system and O solubility in metallic melt increases with a rate of 0.01-0.03 mol./K between 15-21 GPa and 2050-2350 K (Tsuno *et al.*, 2007). For experiments with C added to the starting materials, immiscible melting also occurs (Figs. S-5 and S-6). C contents in the recovered samples are the same as starting materials within uncertainty (Table S-1). This indicates that C does not dissolve into N-rich fluid during immiscible melting.

The combination of *in situ* and *ex situ* analysis was employed to constrain the solubility of N in Fe-N-C alloys (Fig. 2). Near 1 bar in all compositions up to 7.7 wt. % N and 10.0 wt. % C, immiscibility of N-rich supercritical fluid and metallic melt observed *in situ* persists to at least 2273 K, the highest temperature investigated here. Solubility of N in Fe-N-C alloy increases from almost 0 near 1 bar to ~6.8 wt. % N at 6.3 GPa, as the highest pressure investigated here (Fig. 2). The pressure required for closing the miscibility gap increases with the starting N and C contents (Fig. 2). For Fe-1.4 wt. % N starting material at about 0-0.1 GPa, immiscible liquids persist to at least 1980 K, but no immiscible liquids appear at ~1.4 GPa up to 2000 K (Fig. S-6). In contrast, for Fe-7.7 wt. % N starting composition the solvus persists to at least 6.3 GPa (Fig. 2). Adding 5-10 wt. % C in the starting materials expands the pressure range of the solvus by about 2-5 GPa (Fig. 2). This is because C is more siderophilic than N and it expels N from metallic melt to the immiscible fluid.

A recent study also infers the presence of N-rich fluid from Fe-N-C melt based on the *ex situ* analysis of quenched samples (Speelmanns *et al.*, 2018). The trend of their N solubility model is consistent with our data (Fig. 2). However, the C and Pt contaminations up to 12.5 wt. % from sample capsules are not incorporated into their N solubility models (Speelmanns *et al.*, 2018), which may explain the offsets between these two studies (Fig. 2). The presence of immiscible N-rich fluid in silicate-alloy systems has been observed

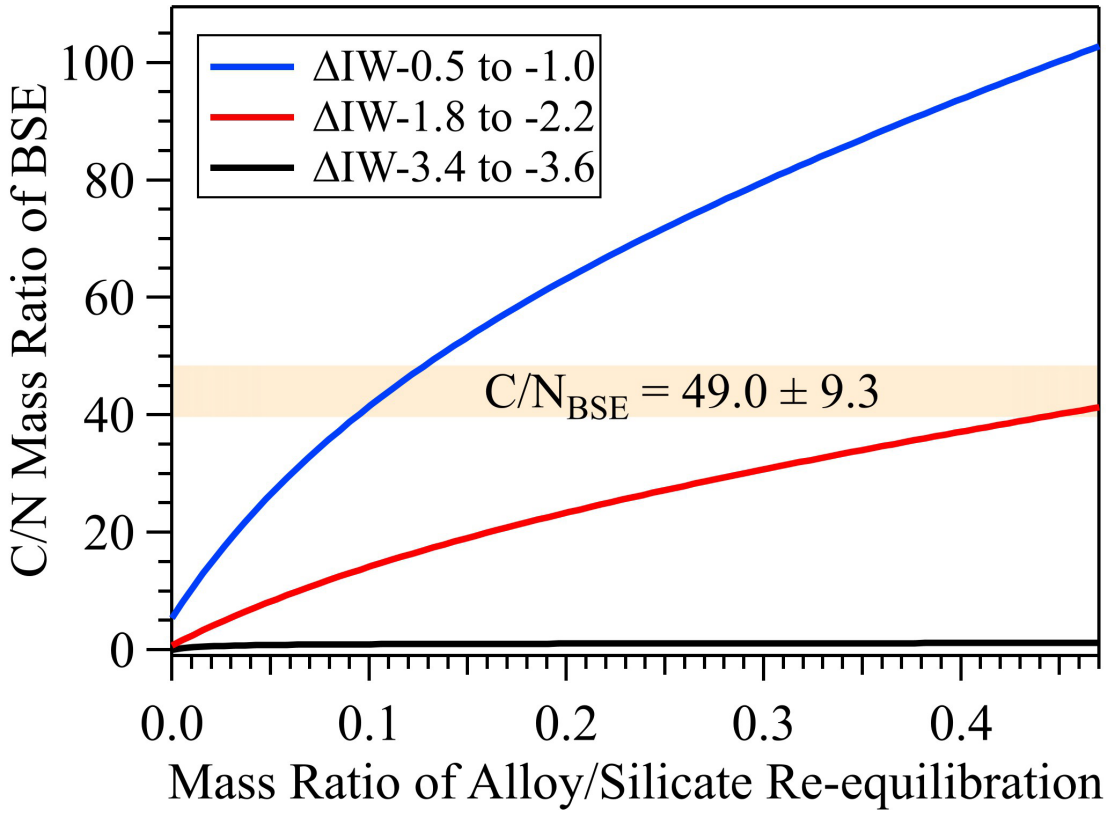

Figure 3 The evolution of the BSE C/N ratio with the degree of re-equilibration between alloy and silicate melts during core formation. The blue curve is calculated at oxidised conditions (ΔIW-0.5 to ΔIW-1.0); the red curve is for reduced conditions (ΔIW-1.8 to ΔIW-2.2) and the black curve is for very reduced conditions (ΔIW-3.4 to ΔIW-3.6). The horizontal yellow bar marks the range of the estimated present BSE C/N ratio (Bergin *et al.*, 2015).

in a previous partitioning study on metallic-silicate melts up to 10 GPa (Roskosz *et al.*, 2013), supporting that this immiscible phenomenon could occur in a realistic magma ocean phase assemblage.

Missing N in the Mantle

The conundrum of missing N in the mantle can be solved by accounting for immiscibility of N in the Fe-N-C system in modelling Earth's N budget. Our model calculates the BSE C/N ratio in three steps (Fig. S-8 and SI): first, we assume Earth-forming impactors have alloy core and silicate mantle in equilibrium with average alloy/silicate mass ratio of 0.46, same as the Earth's core/mantle mass ratio. The amount of N stored in metallic core is controlled by oxygen fugacity (Dalou et al., 2017): 90.2 % N would stay in the core at oxidised bodies (ΔIW-0.5 to -1.0); this number decreases to 69.7 % and 12.1 % at modestly reduced (ΔIW-1.8 to -2.2) and more reduced bodies (ΔIW-3.4 to -3.6), respectively (Fig. S-9). In contrast, previous models assume all C and N are initially stored in silicate (Bergin *et al.*, 2015; Hirschmann, 2016; Dalou *et al.*, 2017). This assumption sets the initial BSE C/N ratio at 25 without loss of the primordial atmosphere, which is about 20-24 higher than our initial BSE C/N ratios (Fig. 3). Secondly, we assume that extensive melting of alloy during high energy impacts induces immiscible melting, resulting in loss of all N stored in impactors' cores to space. In general, the fraction of N released from an impactor depends on the core/mantle mass ratios in the accreting bodies: the degree of melting during accretion/melting, the extent of immiscibility between N-rich supercritical fluid and metallic melt, and the fraction of atmospheric N loss to space. As our model assumes impactor cores melt completely and release N at the magma ocean surface, it yields an upper limit for N loss at this stage. The loss of N results in an extremely high C/N ratio in the metallic phase. Once such N-depleted metallic droplets sink below the depth where solubility of N in alloy increases (Fig. S-8), N could partition from the magma ocean into N-depleted alloy droplets and therefore elevate the BSE C/N ratio as the alloy joins Earth's growing core.

Overall, the loss of N from impactor cores could significantly lower Earth's bulk N budget and therefore raise the BSE C/N ratio (Fig. 3). Because N partitions more strongly into alloy under more oxidised conditions, more N is subject to loss from oxidised accreting bodies (Fig. S-9). Similarly, the subsequent core formation would also result in a higher C/N ratio of the BSE under oxidised conditions (Fig. 3). Over time during core formation, f_{O_2} is estimated to evolve from lower values of ΔIW-3.9 to ΔIW-1.9 to higher values of ΔIW-1.9 to ΔIW-1.0 (Rubie *et al.*, 2011, Badro *et al.*, 2015). Therefore, the BSE C/N ratio is expected to evolve from 0.03-0.5 at very reduced conditions to 0.7-41.4 at reduced conditions and finally to 5-130.0 at slightly reduced conditions (Fig. 3). Compared with previous models (Bergin *et al.*, 2015), our model matches the estimated BSE C/N ratio for an extensive range of redox conditions, the degree of alloy-silicate re-equilibration and extent of loss of nascent atmosphere during accretion and core formation. Notably, both C and N form accessory minerals, such as diamonds, iron carbides and iron/titanium/chromium nitrides (*e.g.*, Fegley, 1983; Javoy, 1997; Kaminsky and Wirth, 2017), which have not been considered in the estimated BSE C/N ratio yet. In addition, the presence of deep mantle carbonates (*e.g.*, Brenker *et al.*, 2007) and high solubilities (10s to 1000s mg/g) of N in transition zone and lower mantle minerals (Yoshioka *et al.*, 2018), both of which are sensitive to redox and pH conditions (*e.g.*, Rohrbach and Schmidt, 2011; Mikhail *et al.*, 2017), would also influence the estimation of the BSE C/N ratio.

Vapourisation during accretion has recently been evoked to explain Mg, Si and Fe isotopic compositions in the BSE (Hin *et al.*, 2017) and the pattern of volatile element depletion (Norris and Wood, 2017), indicating its critical role in the early stage of Earth evolution. Considering the high C/N ratios (>10) of most planetary bodies (Bergin *et al.*, 2015), the C/N ratios of the impactors' cores would be even higher and therefore promote immiscible melting during impact. In addition, for Earth-like planets at the proposed synestia stage (Lock and Stewart, 2017), the magma ocean is surrounded by massive vapourised materials, which are at pressures between 0.1 bar and 1.0 GPa. In this stage, the loss of N through immiscible fluid could significantly shape the BSE C/N ratio.

Acknowledgements

S.M. Dorfman acknowledges funding from Michigan State University, the Sloan Foundation's Deep Carbon Observatory Grant G-2017-9954, and NSF EAR-1751664. J. Li acknowledges partial support from NSF AST 1344133, NASA NNX15AG54G, and Sloan Foundation Deep Carbon Observatory Grant G-2017-9954.

Editor: Simon Redfern

Author Contributions

J. Liu and S.M. Dorfman designed research; J.C. Liu, S.M. Dorfman, M. Lv, J. Li, F. Zhu, Y. Kono performed experiments; J. Liu analysed the data and built the model; J. Liu and S.M. Dorfman wrote the paper.

Additional Information

Supplementary Information accompanies this letter at http://www.geochemicalperspectivesletters.org/article1919.

Cite this letter as: Liu, J., Dorfman, S.M., Lv, M., Li, J., Zhu, F., Kono, Y. (2019) Loss of immiscible nitrogen from metallic melt explains Earth's missing nitrogen. *Geochem. Persp. Let.* 11, 18–22.

References

Alexander, C.M.O., Howard, K.T., Bowden, R., Fogel, M.L. (2013) The classification of CM and CR chondrites using bulk H, C and N abundances and isotopic compositions. *Geochimica et Cosmochimica Acta* 123, 244–260.

Badro, J., Brodholt, J.P., Piet, H., Siebert, J., Ryerson, F.J. (2015) Core formation and core composition from coupled geochemical and geophysical constraints. *Proceedings of the National Academy of Sciences* 112, 12310–12314.

Bergin, E.A., Blake, G.A., Ciesla, F., Hirschmann, M.M., Li, J. (2015) Tracing the ingredients for a habitable earth from interstellar space through planet formation. *Proceedings of the National Academy of Sciences* 112, 8965–8970.

Brenker, F.E., Vollmer, C., Vincze, L., Vekemans, B., Szymanski, A., Janssens, K., Szaloki, I., Nasdala, L., Joswig, W., Kaminsky, F. (2007) Carbonates from the lower part of transition zone or even the lower mantle. *Earth and Planetary Science Letters* 260, 1–9.

Dalou, C., Hirschmann, M.M., von der Handt, A., Mosenfelder, J., Armstrong, L.S. (2017) Nitrogen and carbon fractionation during core–mantle differentiation at shallow depth. *Earth and Planetary Science Letters* 458, 141–151.

Fegley, B. (1983) Primordial retention of nitrogen by terrestrial planets and meteorites. *Journal of Geophysical Research: Solid Earth* 88, A853–A868.

Fei, Y., Brosh, E. (2014) Experimental study and thermodynamic calculations of phase relations in the Fe–C system at high pressure. *Earth and Planetary Science Letters* 408, 155–162.

Grady, M.M., Wright, I.P. (2003) Elemental and Isotopic Abundances of Carbon and Nitrogen in Meteorites. *Space Science Reviews* 106, 231–248.

Grumbach, M.P., Martin, R.M. (1996) Phase diagram of carbon at high pressures and temperatures. *Physical Review B* 54, 15730–15741.

Guillermet, A.F., Du, H. (1994) Thermodynamic Analysis of the Fe-N System Using the Compound-Energy Model with Predictions of the Vibrational Entropy. *Zeitschrift Fur Metallkunde* 85, 154–163.

Halliday, A.N. (2013) The origins of volatiles in the terrestrial planets. *Geochimica et Cosmochimica Acta* 105, 146–171.

Hin, R.C., Coath, C.D., Carter, P.J., Nimmo, F., Lai, Y.-J., Pogge von Strandmann, P.A.E., Willbold, M., Leinhardt, Z.M., Walter, M.J., Elliott, T. (2017) Magnesium isotope evidence that accretional vapour loss shapes planetary compositions. *Nature* 549, 511–515.

Hirschmann, M.M. (2016) Constraints on the early delivery and fractionation of Earth's major volatiles from C/H, C/N, and C/S ratios. *American Mineralogist* 101, 540–553.

Javoy, M. (1997) The major volatile elements of the Earth: Their origin, behavior, and fate. *Geophysical Research Letters* 24, 177–180.

Kaminsky, F., Wirth, R. (2017) Nitrides and carbonitrides from the lowermost mantle and their importance in the search for Earth's "lost" nitrogen. *American Mineralogist* 102, 1667–1676.

Kono, Y., Park, C., Kenney-Benson, C., Shen, G., Wang, Y. (2014) Toward comprehensive studies of liquids at high pressures and high temperatures: Combined structure, elastic wave velocity, and viscosity measurements in the Paris–Edinburgh cell. *Physics of the Earth and Planetary Interiors* 228, 269–280.

Kono, Y., Kenney-Benson, C., Shibazaki, Y., Park, C., Wang, Y., Shen, G. (2015) X-ray imaging for studying behavior of liquids at high pressures and high temperatures using Paris-Edinburgh press. *Review of Scientific Instruments* 86, 072207.

Kowalski, M., Spencer, P.J. (1995) Thermodynamic reevaluation of the C-O, Fe-O and Ni-O systems: Remodelling of the liquid, BCC and FCC phases. *Calphad* 19, 229–243.

Liu, J., Li, J., Hrubiak, R., Smith, J.S. (2016) Origins of ultralow velocity zones through slab-derived metallic melt. *Proceedings of the National Academy of Sciences* 113, 5547–5551.

Lock, S.J., Stewart, S.T. (2017) The structure of terrestrial bodies: Impact heating, corotation limits, and synestias. *Journal of Geophysical Research: Planets* 122, 2016JE005239.

Marty, B. (2012) The origins and concentrations of water, carbon, nitrogen and noble gases on Earth. *Earth and Planetary Science Letters* 313–314, 56–66.

Mikhail, S., Barry, P.H., Sverjensky, D.A. (2017) The relationship between mantle pH and the deep nitrogen cycle. *Geochimica et Cosmochimica Acta* 209, 149–160.

Norris, C.A., Wood, B.J. (2017) Earth's volatile contents established by melting and vaporization. *Nature* 549, 507–510.

Rohrbach, A., Schmidt, M.W. (2011) Redox freezing and melting in the Earth's deep mantle resulting from carbon-iron redox coupling. *Nature* 472, 209–212.

Roskosz, M., Bouhifd, M.A., Jephcoat, A.P., Marty, B., Mysen, B.O. (2013) Nitrogen solubility in molten metal and silicate at high pressure and temperature. *Geochimica et Cosmochimica Acta* 121, 15–28.

Rubie, D.C., Frost, D.J., Mann, U., Asahara, Y., Nimmo, F., Tsuno, K., Kegler, P., Holzheid, A., Palme, H. (2011) Heterogeneous accretion, composition and core–mantle differentiation of the Earth. *Earth and Planetary Science Letters* 301, 31–42.

Speelmanns, I.M., Schmidt, M.W., Liebske, C. (2018) Nitrogen Solubility in Core Materials. *Geophysical Research Letters* 45, 7434–7443.

Tsuno, K., Ohtani, E., Terasaki, H. (2007) Immiscible two-liquid regions in the Fe–O–S system at high pressure: Implications for planetary cores. *Physics of the Earth and Planetary Interiors* 160, 75–85.

Yoshioka, T., Wiedenbeck, M., Shcheka, S., Keppler, H. (2018) Nitrogen solubility in the deep mantle and the origin of Earth's primordial nitrogen budget. *Earth and Planetary Science Letters* 488, 134–143.